Journal of Population Therapeutics & Clinical Pharmacology

RESEARCH ARTICLE
DOI: 10.53555/jptcp.v31i5.6377

SYNTHESIS AND CHARACTERIZATION OF NANOPARTICLES FOR THE REMOVAL OF HEAVY METALS FROM DRINKING WATER OF DAMS IN BALOCHISTAN

Mohammad Shoiab Khan[1], Manzoor Iqbal Khattak[2*], Nida Kazmi[3], Adnan Afridi[4], Munnaza Saeed[5] and Hamid Ullah[6]

[1-5]Chemistry Department, University of Balochistan, Quetta, Pakistan
[6]Chemistry Department, Balochistan Universty of Information, Technology, Engineering and Management Sciences, Quetta, Pakistan

***Corresponding Author:** Manzoor Iqbal Khattak
Email address: manzoor_iqbal@yahoo.com

Abstract
The aim of this research was to investigate the waters of Balochistan dams as a reference for extracting various heavy metal ions. Among the water sources for these dams are shallow groundwater (SG), runoff from a seasonal floodplain rich in lithological rocks, including NaCl, as well as the discharge of effluents and residential wastes (inorganic contaminants). ZnO particles were synthesized using solid precipitation techniques. The average dimensions of the rod-shaped ZnO particles were 497.34 ± 15.55 nm in length and 75.78 ± 10.39 nm in diameter. These particles exhibited efficient extraction, eliminating over 85% of heavy metal ions such as Cu(II), Ag(I), and Pb(II) after an hour of UV exposure. However, for ions like Cr(VI), Mn(II), Cd(II), and Ni(II), the ectraction rate was less than 15%. The elimination procedures involved the adsorption of metals through oxidation and reduction. Evaporation significantly influenced the surface groundwater in the saline floodplain, which is periodically transported to the Balochistan dams, as revealed by analyses of water type evolution and surface hydrology. The research region in the present study is typically mildly acidic or mildly alkaline, with the majority of samples aligning with guidelines set by the World Health Organization. However, prolonged usage of this water, given its high salinity, may have a negative effect on soil and grape yield.

Keywords: Material Science; Nanotechnology; Environmental Pollution; Drinking water,

1. Introduction

A worldwide revolution in nanotechnology has resulted in the emergence of new words during the last ten years, including nanosciences, nanotechnologies, nanomaterials, nanostructures, and nanoparticles. The creation of components, structures, and gadgets at the nanoscale in different sophisticated technological sectors is the main emphasis of this revolution, which is the basic need of this modern era of science and technology.

Advanced sciences that study nanoscale phenomena are also used in current attempts to comprehend nanosciences and technology at the atomic level. According to Ozin *et al.* (2006), Guozhong (2004), and Roduner (2006), these nanomaterials represent a brand-new technical field that is centered on designing, cultivating, and employing small-sized elements based on a fundamental understanding

of the relationship between the properties of physical and chemical phenomena and the dimensions of the elements.

Chemistry is an area where nanoscience and technology are very important. To produce tiny building components with various sizes, forms, compositions, and structural surfaces, chemical techniques must be used. These structural pieces may serve a purpose on their own or as an integral component of bigger constructions with particular purposes and uses (Ozin *et al.*, 2006).

According to Tiwari *et al.* (2012) and Pokropivny *et al.* (2008), nanostructural materials (NSMs) are small-scale materials with nano-sized structural units in at least one dimension that display size-dependent effects. These materials, therefore, have improved surface effects. The total surface area rises noticeably as the size of the pieces becomes smaller because the surface area grows in proportion to the same volume of material.

Numerous NSMs have been created during the last 20 years, demanding categorization. According to their constituents, NSMs may be classified into four groups: 0D, 1D, 2D, and 3D, (Pokropivny *et al.*, 2008). In accordance with this categorization, 3D structures are not regarded as nanostructures since they must have dimensions greater than 100 nm. However, 3D structures that include 0D, 1D, and 2D nanoparticles may be categorized as nanomaterials (Pokropivny *et al.*, 2008).

1.1. Heavy Metals

Although there isn't a clear definition of the phrase "heavy metals" (HM) in the literature currently in print, it has been commonly used in recent years (Duffus, 2002). Bjerrum's Inorganic Chemistry (Foster, 1936), which was published in 1936, has one of the oldest references to the phrase "heavy metal" in literature (Nordberg *et al.*, 2007). According to several standards, heavy metals are defined as having a density larger than 7 g/cm^3 (Duffus, 2002; Nordberg *et al.*, 2007; Hashim *et al.*, 2011; Fu *et al.*, 2011). However, historical knowledge of metals leads one to believe that specific gravity is not a major factor in the reactivity of metals (Duffus, 2002). The application of other definitions, which are based on atomic weight, is still constrained (Patterson *et al.*, 1987). However, this method falls short when identifying heavy metals that are frequently utilized in industry without taking into account their toxicity (Duffus, 2002).

1.2. Adsorption

Adsorption, which is often utilized to extract chemicals from fluid phases, is defined as the buildup of compounds on a material's surface (Kammerer *et al.*, 2011; Worch, 2012). Chemical make-up, physical characteristics, and polarity all serve as classification criteria for adsorbent materials. They also differ in terms of density, porosity, surface area, and particle size.

Adsorption, when employed to extract pollutants, does not create undesirable byproducts. Due to its straightforward design and operation, it is often chosen over other water treatment techniques (Lofrano, 2012). Pollutant dispersion via transport, particle surface adsorption, and pollutant transport inside the adsorbent material are the three phases of the adsorption process. Each step is dependent on the characteristics of the solid particles (Barakat, 2011).

Water is a precious yet finite resource that is in danger. It is necessary for sustaining progress, the environment, and life. 97% of the salt water on earth is found in the seas (Tressaud, 2006). Humans consume the majority of freshwater, which makes up just 3% of all water (WHO, 2011).

Drinking water supply is becoming more and more limited, and water quality has been a persistent problem. Human activities and the expanding population both contribute to the sharp rise in water usage.

Human health may be endangered by contaminated water that contains elements including F, As, NO_3, Fe, Mn, Cl, Se, toxic metals, and radioactive compounds from anthropogenic or natural sources (Jadhav *et al.*, 2015). Due to its detrimental effects on the ecology and water quality, which affect many people, wastewater has been a serious concern. As a result, several techniques for wastewater purification have been developed. Pollutant ectraction from water may minimize the dangers to people and the environment while also enhancing ecosystem health, public health, and water quality. It can also safely restore water to natural reservoirs.

The rise of illnesses like diarrhea and cholera has been attributed to poor water quality in many undeveloped towns, including Quetta in Balochistan. This demonstrates how the necessary agencies have failed to supply citizens with clean drinking water. Many people depend on groundwater supplies, which often have excessive fluoride levels and may lead to serious illnesses. In response, Quetta's government has experimented to ascertain the amount of fluoride in water supply plans.
In cities like Quetta, the problem of delivering clean, drinkable water is often related to the low quality of the water resources, demanding suitable treatment. Water treatment in poor nations has a number of difficulties, such as: • High investment costs, including operation and maintenance costs; • Requirements for sophisticated equipment and processes; • Environmental issues, including the disposal of garbage. The development of efficient and affordable technology is essential for delivering clean water due to budgetary limitations (Pollard *et al.*, 1994).
In this work, the extraction of ions through particles of ZnO using visible light and UV conditions from an aqueous solution has been evaluated. Particles of ZnO are inferred based on each metal ion extraction process, as well as the examination of the byproducts.

2. Materials and Method

2.1. Area of Study

Water samples were collected in 1-2 liter polyethylene bottles from various dams (Sabakzai, Hub, Mirani, and Akra Kaur) in Balochistan during the months of October and November 2022.

2.2. Synthesis of ZnO nanoparticles

A 0.5% soluble starch solution was prepared by dissolving it in 500 ml of distilled water and heating it in a microwave oven (Samsung, NoCE103VD) for complete solubilization. Subsequently, 14.874 g (0.1 mol) of zinc nitrate was added to the solution. The mixture was then stirred continuously with a magnetic stirrer (Tarson digital spinning) at room temperature for one hour. After the complete dissolution of zinc nitrate, 300 ml (0.2 mol) of sodium hydroxide solution was added dropwise to the mixture while stirring and avoiding contact with the container walls. The reaction was allowed to proceed for an additional 2 hours after the sodium hydroxide was added.
Following the reaction, the mixture was left to stand overnight, and the supernatant solution was carefully decanted. The remaining solution was then centrifuged at 10,000 g using a Remi cooling centrifuge device (model No-C30BL) to separate the nanoparticles, and the supernatant was discarded. The produced nanoparticles were washed three times with distilled water to remove any byproducts and excess starch attached to the particles. After washing, the nanoparticles were dried overnight at 80°C. During the drying process, the full conversion of $Zn(OH)_2$ into ZnO occurred, as depicted in Figure 2.1.

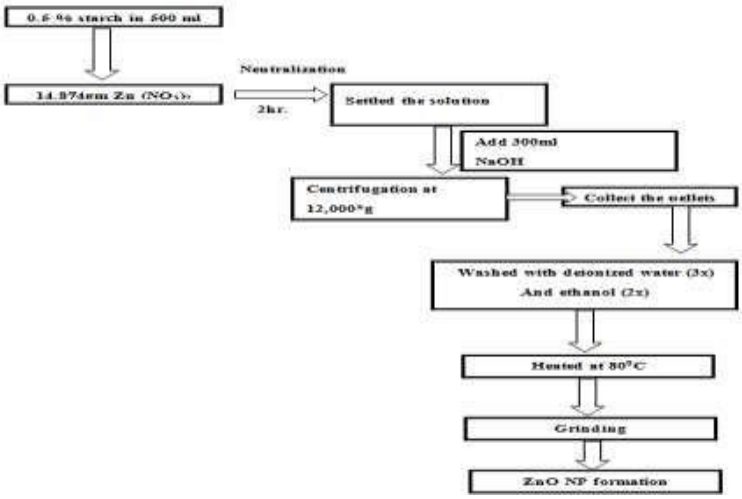

Figure2.1. Schematic diagram for the synthesis of ZnO nanoparticles.

2.3. Adsorption of Heavy Metal Ions Using Nanotechnology:

In each experiment, ZnO particles (1 g/l) were added to a 50 ppm single-element solution and magnetically stirred in the dark for 30 minutes to achieve adsorption/desorption equilibrium. Thereafter, the light source for the photocatalytic process was activated. Using ICP-OES, metal concentrations were measured after every 15 min interval. The equation given below was used to calculate the extraction efficiency of ions by ZnO particles (2.1).

$$\eta\,(\%) = \left(\frac{Co - Ct}{Co}\right)100 \text{ ---------- (2.1)}$$

Where Co and Ct are the initial concentration and the concentration after time t of metal ions.

2.4. Characterizations: An X-ray diffractometer was used for the analysis of Zno particles (crystal structures) with a Cu-K (copper-monochromatic) radiation source. The XRD spectrum was matched with the Joint Committee on Powder Diffraction Standards (JCPDS) database. The High Resolution Transmission Electron Microscope (HRTEM) image was obtained by the Tecnai G220 S-Twin. Elemental distribution of metal on ZnO was performed by using an Energy Dispersive X-ray (EDX) mapping analysis.

2.5. Data Analysis: Statistical analysis was performed using the latest Statistical Program for Natural Sciences (SPNS) software.

3. Results and Discussion

3.1. ZnO Particles (metals elimination efficiency)

ZnO particles eliminated heavy metal ions with varied efficiency after 1 hour of irradiation. Regardless of light source, ZnO particles eliminated 100% of Cu (II) ions, but Mn, Cd, and Ni ions were eliminated up to 9.00%, only as shown in Figures 3.1(a) and (b).

ZnO particles used photocatalytic reduction to remove Ag (I) ions, but only when exposed to UV light, with extraction up to 97.92% (light sources i.e. optical excitation sources). The physical adsorption of Pb (II) ions by ZnO particles exposed to visible light was only 62.65%. UV light enhanced removal effectiveness to 85.18%, showing that photocatalytic reduction may operate with physical adsorption.

ZnO particles exposed to visible light physically adsorb Cr (VI) ions from the solution with 43.34% effectiveness. UV light drastically reduced removal efficacy to 14.83% due to physical adsorption. According to further tests, ZnO particles remove Cr (VI) ions in Subsection 3.3. These findings are summarized in Table 3.1.

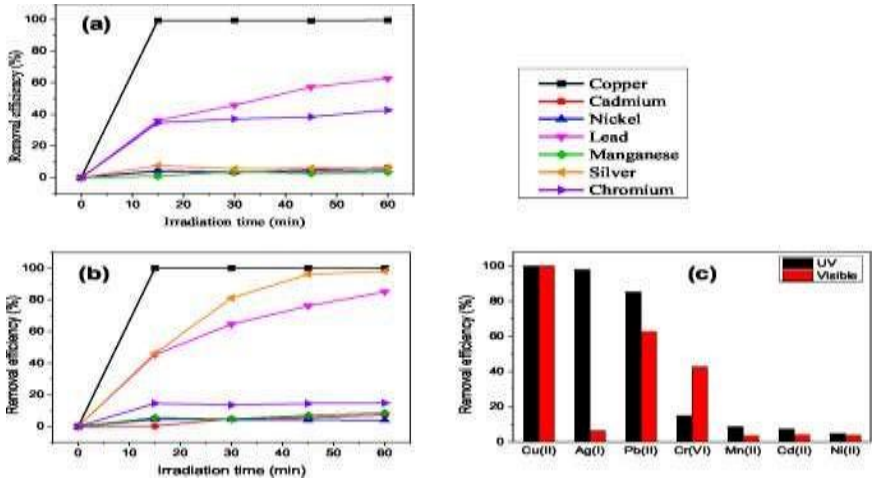

Figure 3.1. Metals ions extraction efficiency (a) visible light, (b) UV light and (c) metal ions (after 1-hr) extraction efficiency by ZnO particles.

Table 3.1. Lists the effectiveness of ZnO particles for extracting heavy metal ions with possible extraction processes.

Heavy metal ions	Removal Efficiency			Possible Removal Mechanism
	Visible / Dark	UV	Trend	
Ag (I)	Poor	Good	↑	A + R/O
Cr (VI)	Moderate	Poor	↓	A + R/O
Pb (II)	Moderate	Good	↑	A + R/O
Mn (II)	Poor	Poor	No significant change	A
Cu (II)	Good	Good	No significant change	A
Cd (II)	Poor	Poor	No significant change	A
Ni (II)	Poor	Poor	No significant change	A
Legends: Adsorption e A, Reduction e R, Oxidation e O				

3.2 Characteristics of M/ZnO hybrid particles' structures

Hexagonal ZnO structures include diffraction peaks at 31.09°, 33.77°, 35.56°, 46.89°, 55.96°, 62.27°, 65.79°, 68.51°, 76.41°, and 89.09°. ZnO's conventional lattice constants are a = 3.25 and c = 5.21 nm. Each M/ZnO hybrid particle had unrelated X-ray diffraction peaks (Figures 9(a) and 10(a). Figures 3.2 (b) and 3.3 (b) show Cu/ZnO hybrid particle XRD patterns. The CuO phase had additional (002), (020), and (202) planes at UV and visible light diffraction peaks of 35.6°, 56.3°, and 61.1°. CuO crystals (JCPDS card number 98-005-9312) were monoclinic based on diffraction peaks.

After visible light exposure, Ag/ZnO hybrid particles displayed only ZnO-specific diffraction peaks (Figure 3.2(c)). UV light revealed a (111) and (112) plane in Ag/ZnO hybrid particles. UV light did not add diffraction peaks to Ag/ZnO hybrid particles. Ag on ZnO particles was too tiny for XRD to detect, as illustrated in Figure 3.3 (c).

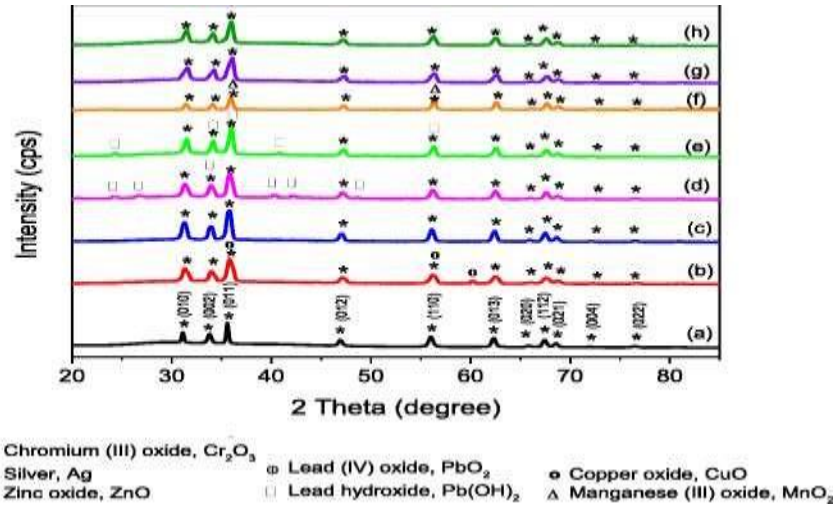

Figure 3.2. X-ray diffractograms of ZnO with light exposed heavy metals deposition (a) ZnO particles,(b) Cu/ZnO, (c) Ag/ZnO, (d) Pb/ZnO, (e) Cr/ZnO, (f) MnO, (g) Cd/ZnO, and (h) Ni/ZnO hybrid particles.

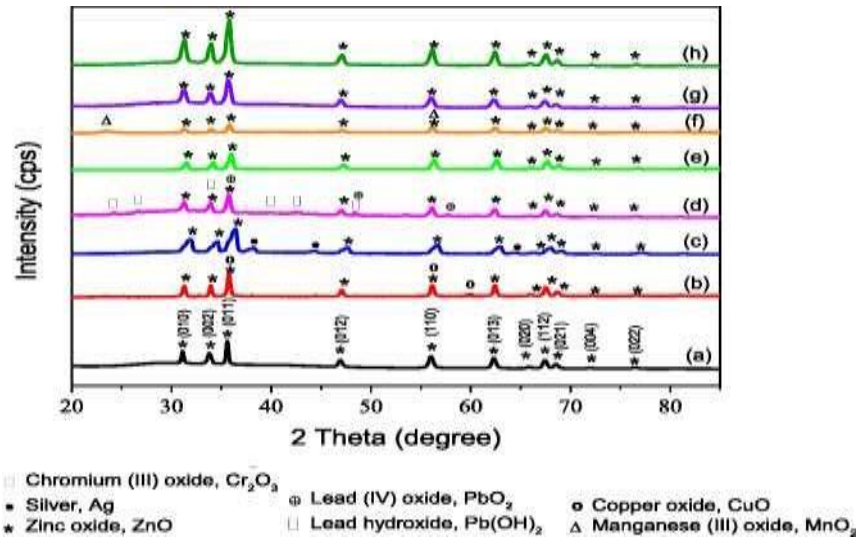

Figure 3.3. ZnO X-ray diffractograms of (a) ZnO particles, (b) Cu/ZnO, (c) Ag/ZnO, (d) Pb/ZnO, (e) Cr/ZnO, (f) Mn/ZnO, (g) Cd/ZnO, (h) Ni/ZnO hybrid particles. The adsorption of these heavy metals were carried out at UV radiation.

And (222) at diffraction peaks of 38.29°, 44.49°, and 64.52° related to Ag^{+3} structure (JCPDS Card #98-008-3900) as shown in Figure 3.3 (c). The results proposed that deposition of Ag, if there was any, should be limited by XRD.

Figures 3.2(a) and 3.3(a) exhibit M/ZnO hybrid particle XRD patterns following heavy metal ion extraction. Diffraction peaks at various angles correspond to hexagonal ZnO crystal surfaces. M/ZnO hybrid particles had additional diffraction peaks. $Pb(OH)_2$ phase was observed in Pb/ZnO hybrid particles generated by both visible and UV methods, but only UV-irradiated particles had PbO_2 XRD peaks (Figures 3.2(b) and 3.3(b,c). Cr/ZnO hybrid particles, when subjected to visible light, showed the Cr_2O_3 phase. However, when exposed to UV light, as shown in Figures 3.2(e) and 3.3(e), no additional diffraction peaks were found. As demonstrated in Figure 3.3(f), only UV-exposed Mn/ZnO hybrid particles had additional peaks in the XRD patterns for the cubic MnO_2 structure. Figures 3.2(g), 3.3(g), 3.2(h), and 3.3(h) show ZnO particles, whereas Cd/ZnO and Ni/ZnO hybrid particles show no crystal structural alterations. XPS investigation confirmed the existence of distinct elements on M/ZnO hybrid particles and found matched binding energies; similar findings was also reported by Munawar *et al.* (2017).

The mechanism of metals and metal oxides on the surfaces of ZnO particles after the adsorption of metal ions under UV light irradiation was further estimated by the process of XPS analysis as shown in Figure 3.4-3.9.

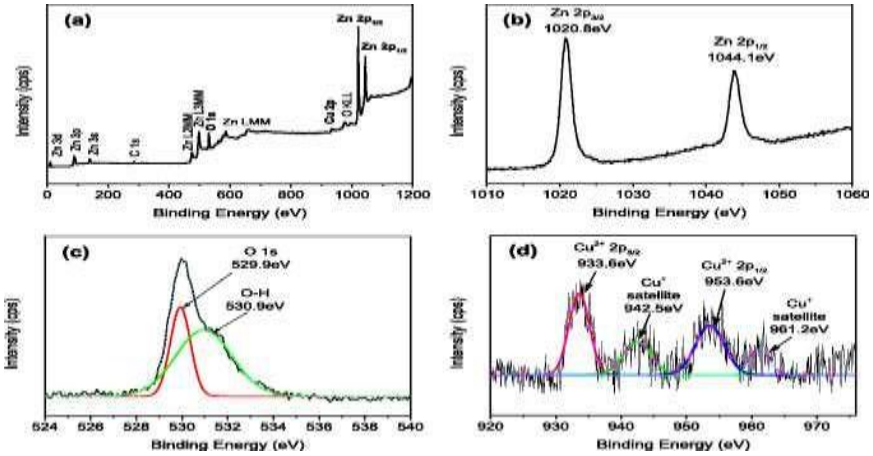

Figure 3.4. Cu-Zn-O nanoparticles with XPS. (a) Zn 2p, (b) O 1s, and (d) Cu 2p energy levels.

XPS spectra study shows Ag, O, Zn in Ag/ZnO hybrid particles (Figure 3.4-3.9) which agree with previous results of XRD. Moreover, the whole study of XPS show the existence of Zn, O, and Ag elements in the hybrid particles of Ag/ZnO, which stresses on the deposition of Ag particles onto the ZnO particles.

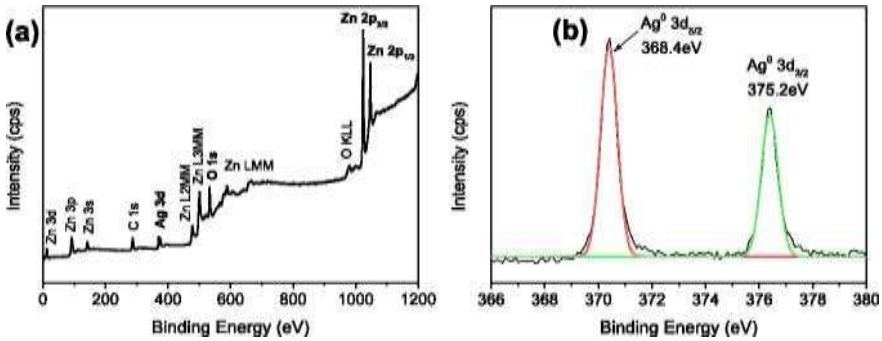

Figure 3.5. XPS of hybrid Ag/ZnO particles (a) A wide sweep, (b) a close inspection.

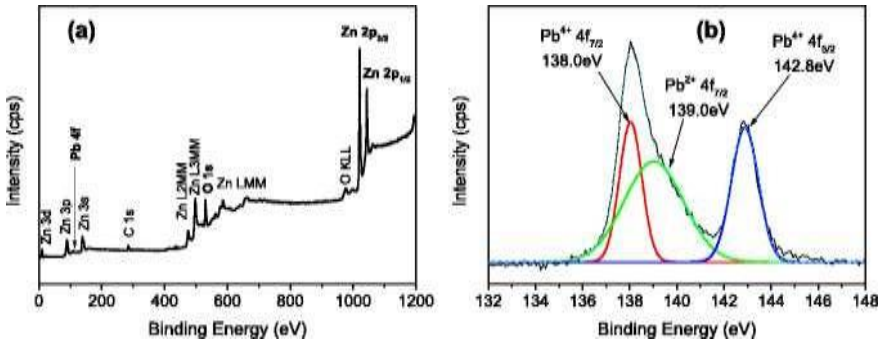

Figure 3.6. XPS of mix of Pb and ZnO with (a) A broad sweep, and (b) a detailed examination.

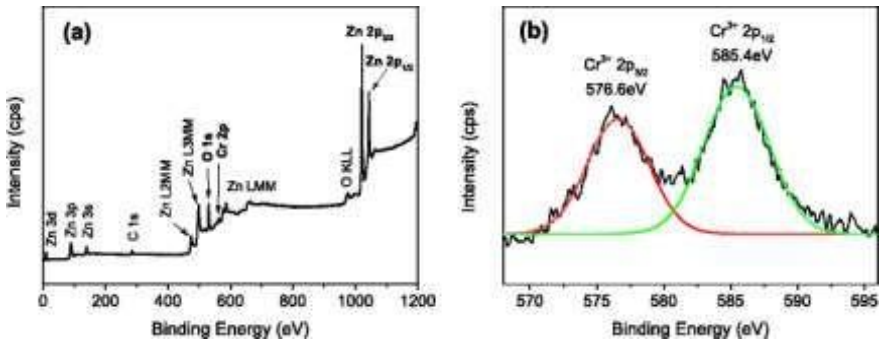

Figure 3.7. XPS of Cr/ZnO particles showing (a) A broad sweep, and (b) a detailed examination.

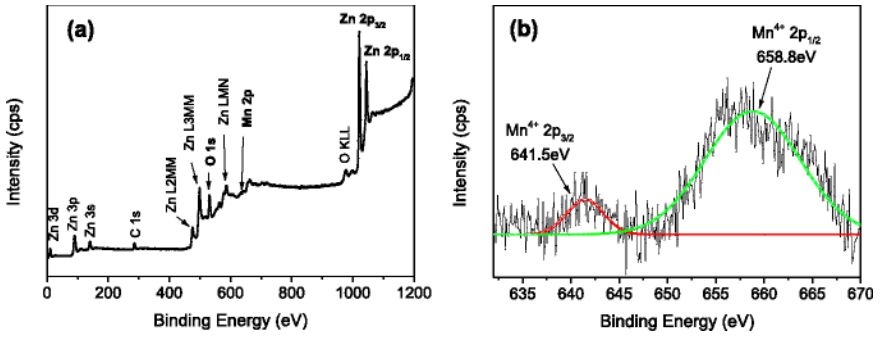

Figure. 3.8. XPS of Mn/ZnO X-ray showing (a) A broad sweep, and (b) a detailed examination.

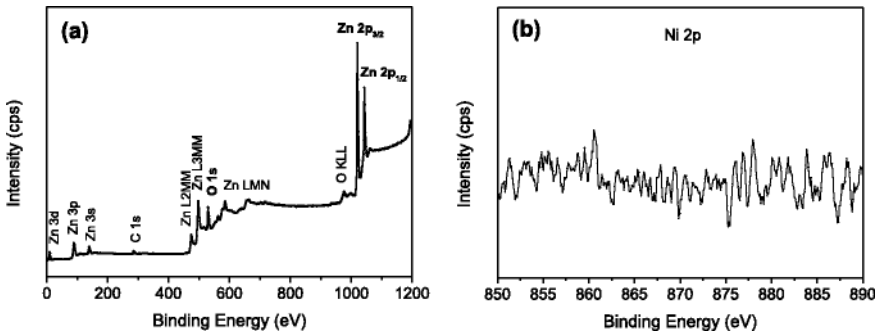

Figure 3.9. XPS of Ni/ZnO particles showing (a) A broad sweep, and (b) a detailed examination.

While it is observed that there is very poor extraction efficiency in cases of Cd and Ni on the surfaces of ZnO.

SEM examined particle morphology. ZnO particles had a rod-like shape and averaged 497.34 15.55 nm and 75.78 10.39 nm (Figure 3.10(a). The rough-surfaced Cu/ZnO hybrid particles had an average diameter and length of 105.11±13.76 nm and 627.22 ±16.69 nm, respectively (Figure 3.10(c). Plate-like Pb/ZnO hybrid particles had an average diameter of 95.56 ± 16.18 nm and a length of 520.32 ± 14.86 nm (Figure 3.10(d)). Figure 3.10(e) shows plate-like Cr/ZnO hybrid particles with an average diameter of 104.99 ±12.52 nm and length of 519.95 ± 13.05 nm. Figure 3.10(f) shows Mn/ZnO hybrid particles with surface particles having an average diameter of 94.37 ± 10.60 nm and a length of 566.82 ± 15.65 nm. Similarly, all these particles on the surfaces of ZnO (nanoparticles) show the extraction of heavy metal particles from the water.

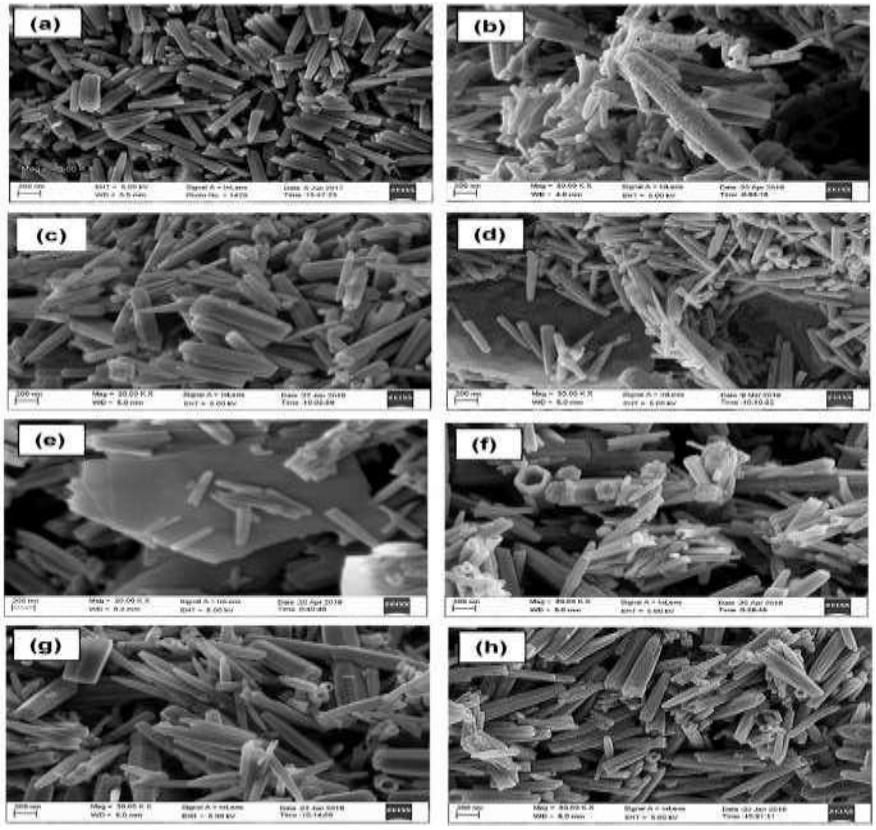

Figure 3.10. SEM images of pure (a) ZnO, (b) Cu/ZnO, (c) Ag/ZnO, (d) Pb/ZnO, (e) Cr/ZnO, (f) Mn/ZnO, (g) Cd/ZnO, and (h) Ni/ZnO hybrid particles under visible light.

Figure 3.11 shows SEM images of ZnO hybrid particles after UV-induced heavy metal ion elimination. As seen in Figure 3.11(a), Cu (II) ions deposited on ZnO particles gave the hybrid particles a rough surface. Cu/ZnO hybrid particles averaged 764.35 11.39 nm long and 145.49 10.02

nm wide. Figure 3.11(b) shows UV-exposed Ag/ZnO hybrid particles in SEM. Ag/ZnO hybrid particles averaged 577.21 ± 13.53 nm long and 102.28 ± 12.54 nm wide. Photo-reduction of Ag^{+} ions on ZnO particles produced tiny particles smaller than 20 nm in diameter. Plate-shaped precipitates were found in Pb/ZnO hybrid particles (Figure 3.11(c)). Figure 3.11(d) shows that the Cr/ZnO hybrid particles did not show the deposited particles.

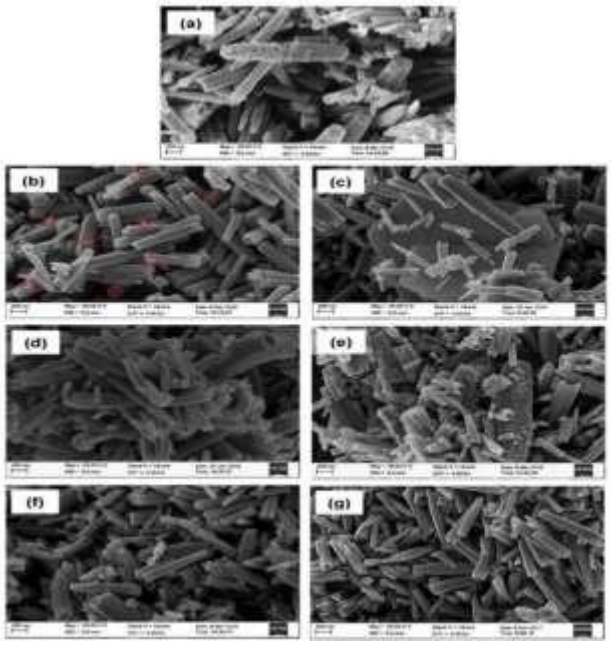

Figure 3.11. SEM images of pure (a) Cu/ZnO, (b) Ag/ZnO, (c) Pb/ZnO, (d) Cr/ZnO, (e) Mn/ZnO, (f) Cd/ZnO, and (g)Ni/ZnO with hybrid particles under UV light.

Average size of Cr/ZnO particles was 99.36 ± 6.58 and 594.01 ± 10.75 nm. As seen in Figure 3.11(e), particle deposition enlarged ZnO particles. Mn/ZnO hybrid particles had average diameters of 110.84 ±10.98 and 579.92 ± 17.31 nm. SEM images concealed Cd (II) and Ni (II) ion deposition in Figure 3.11(f) and (g).

Figure 3.11 shows that UV light affected ZnO particles' capacity to adsorb heavy metal ions more than visible light. Figure 3.12(a) shows the deposition of the foreign layer covered the Cu/ZnO hybrid particle. Fig. 3.12(b) shows a HRTEM picture of the deposition of a Cu-O layer with 0.25 nm lattice fringes onto ZnO particles, corresponding to monoclinic CuO's (002) plane. EDX mapping in Figure 3.12(c)-(e) shows that ZnO particles have abundant Cu element.

Ag particles were visible on ZnO particles in Figure 3.12(a). Ag particles are under 25 nm. The HRTEM picture in Figure 3.12(b) shows that ZnO and Ag particles had lattice fringes of 0.26 and 0.23 nm, respectively. These inter-planar lengths separate the wurtzite ZnO phase's (002) plane from the cubic Ag phase's (111) plane. EDX analysis confirms Ag particles on ZnO particles in Figure 3.12(c)-(e). These results match XRD and XPS.

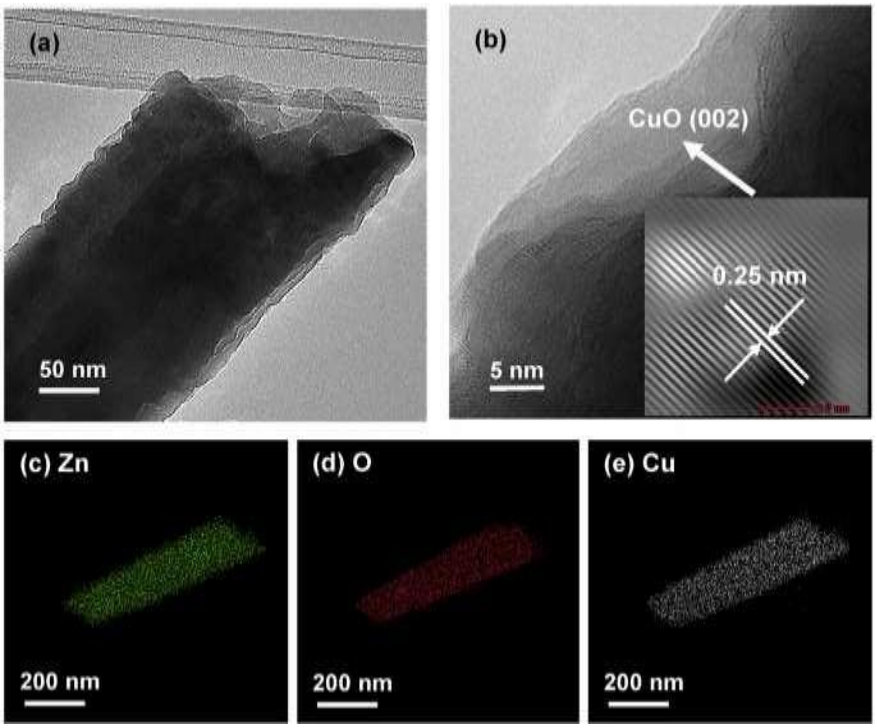

Figure 3.12. After Cu (II) is removed from ZnO particles using UV irradiation, the images of TEM (a), HRTEM (b), and EDX mapping of elements (c), (d), and (e), respectively.

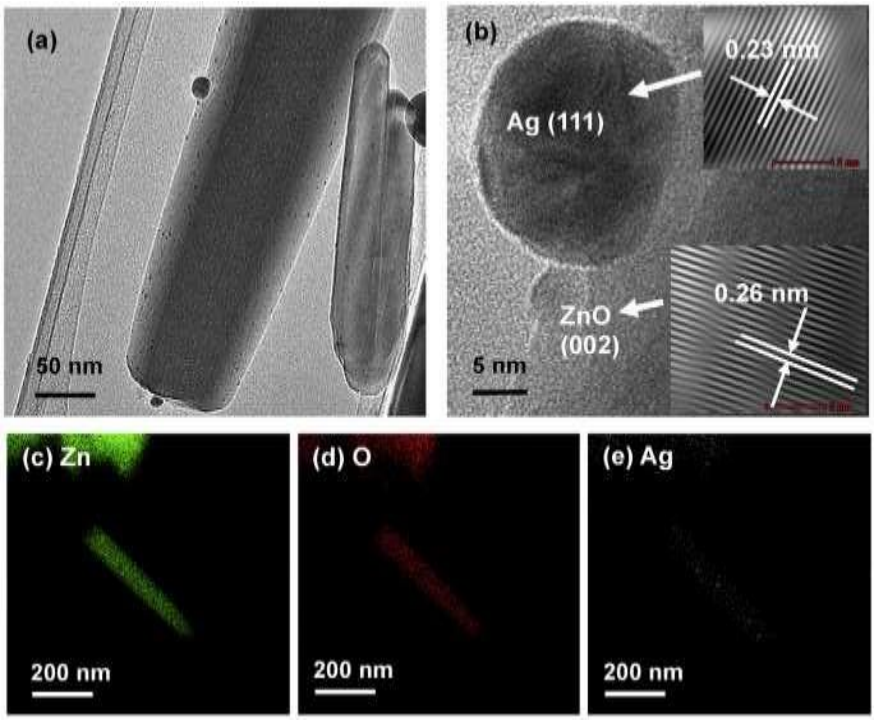

Figure 3.13. UV irradiation removes Ag (I) from ZnO particles, as shown in (a) TEM pictures, (b) HRTEM images, and (c) EDX mapping of (d) Zn, (e) O, and (f) Ag elements.

Pb/ZnO hybrid particles are plate-like in Figure 3.13(a). $Pb(OH)_2$ and PbO_2 crystal grains made up the plate-like structure (Figure 3.13(b)). $Pb(OH)_2$'s (011) plane had 0.32 nm lattice spacing, whereas PbO_2's (110) plane had 0.28. Plate-like structures showed solution crystallization and nucleation. EDX mapping showed a significant concentration of Pb and O in the plate-like structure (Figure 3.13(c)-(e)).

In Figure 3.14(a)-(b), hybrid particles after UV light irradiation did not show Cr particle deposition on ZnO particles. The HRTEM picture of Cr/ZnO hybrid particles showed good crystalline quality. Figure 3.14(c)-(e) confirm that ZnO particle catalysts reduced Cr (VI).
HRTEM micrographs showed small particles of MnO_2 cubic phase and ZnO hexagonal phase (Figure 3.15(a-b). EDX mapping showed that Mn was present in several ZnO particle sizes (Figure 3.15(c)-(e)).

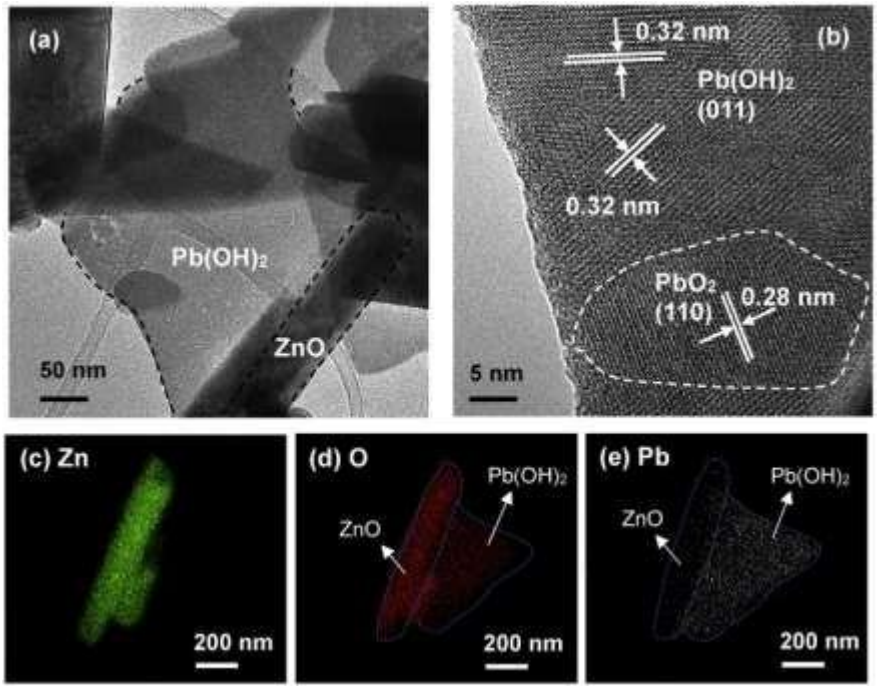

Figure 3.14. ZnO particles with Pb (II) extracted by UV irradiation.

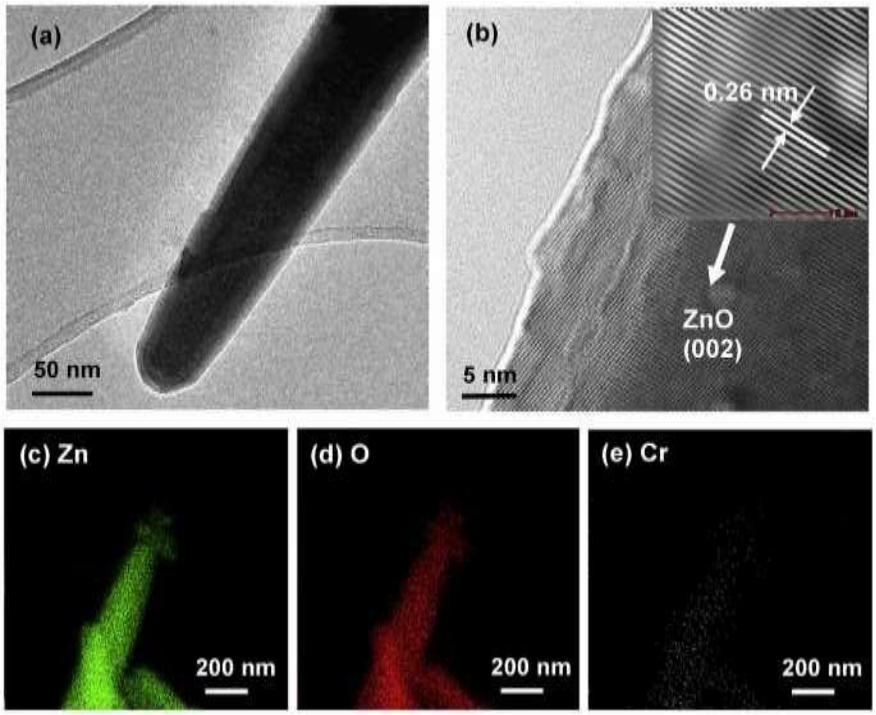

Figure 3.15. After UV irradiation, Cr (VI) is extracted from ZnO particles.

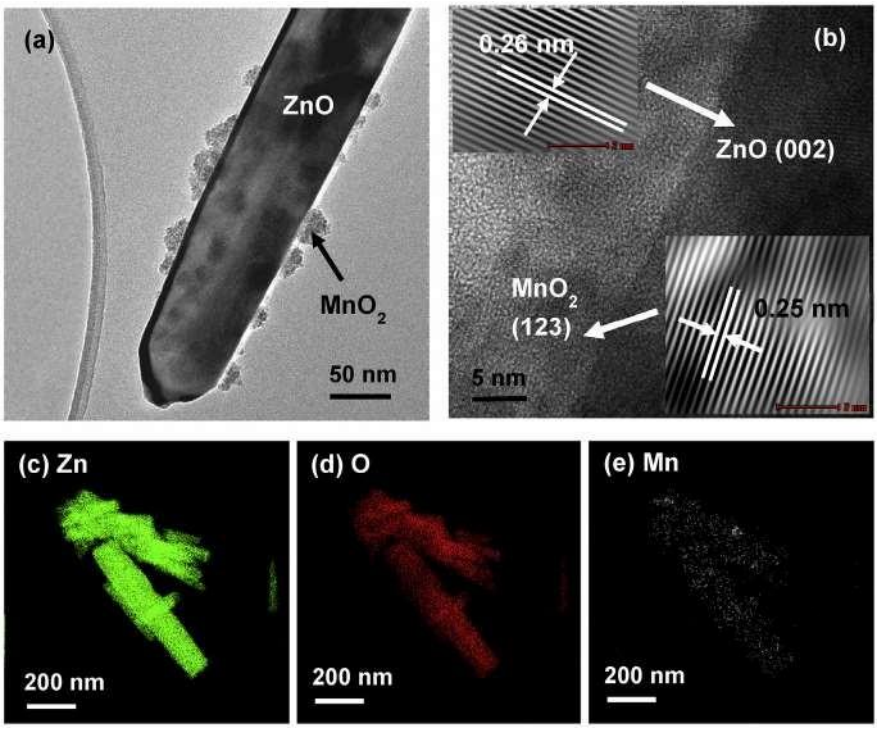

Figure 3.16. UV irradiation extracted Mn (II) from ZnO particles.

As illustrated in Figures 3.16(a) and 3.17(a) Cd (II) and Ni (II), TEM morphological study under UV illumination indicated Cd (II) and Ni (II),
HRTEM images of hybrid particles (Figures 3.10(b) and 3.11(b)) revealed the hexagonal phase of ZnO, which was indexed as the (002) plane. Figures 3.17(c)–24(e) and 25(c)–25(e) exhibit Cd and Ni EDX mapping findings on ZnO particles. Metal and metal oxide deposition and removal methods on ZnO particle surfaces when exposed to UV light as shown in Table 3.2.

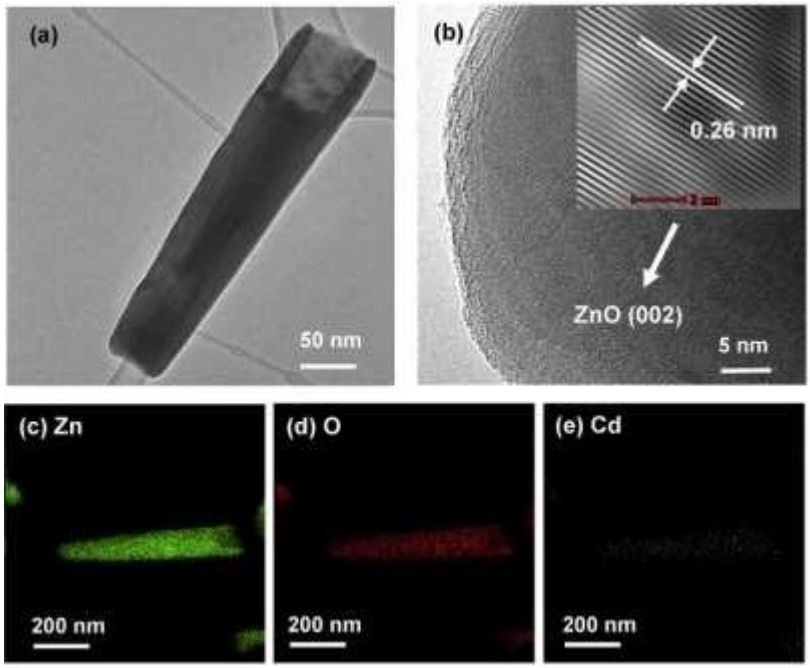

Figure 3.17. After UV irradiation, Cd (II) is removed from ZnO particles.

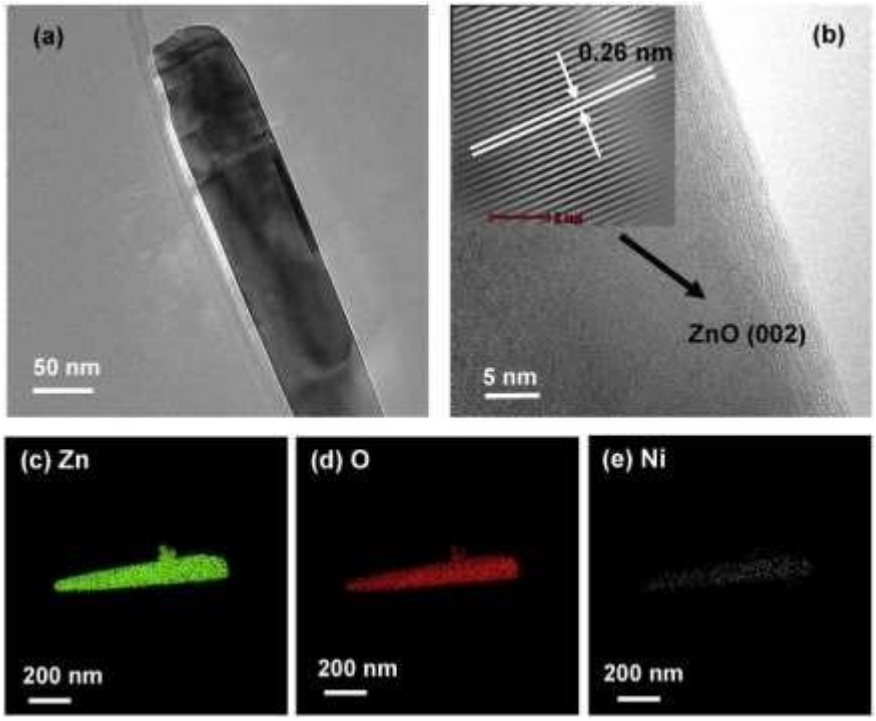

Figure 3.18. Ni (II) removal from ZnO particles using UV irradiation.

Table 3.2. Metal and metal oxide deposition and removal methods on ZnO particle surfaces when exposed to UV light.

Hybrid particles	XPS	XRD		SEM		TEM	HRTEM	EDX mapping	Types of deposits	Dominant removal mechanism
	UV	UV	Visible	UV	Visible	UV				
Ag/ZnO	Ag	Ag	-	Particles	-	Particles	Ag particles	Ag	Ag particles	Reduction
Cr/ZnO	Cr_2O_3	-	Cr_2O_3	-	Flake-like	-	-	Cr	Cr_2O_3 particles	Reduction
Pb/ZnO	PbO_2	$Pb(OH)_2$	$Pb(OH)_2$	Flake-like	Flake-like	Flake-like	$Pb(OH)_2$	Pb, O	$Pb(OH)_2 + PbO_2$ flakes	Oxidation
	$Pb(OH)_2$	PbO_2					PbO_2			
Mn/ZnO	-	MnO_2	-	Particles	Particles	Particles	MnO_2	Mn, O	MnO_2 particles	Oxidation
Cu/ZnO	CuO	CuO	CuO	Rough surface	Rough surface	Thin Film	CuO	Cu, O	CuO thin film	Adsorption
	Cu_2O								Cu_2O	Reduction
Cd/ZnO	-	-	-	-	-	-	-	Cd	Cd thin film (if any)	Adsorption
Ni/ZnO	-	-	-	-	-	-	-	Ni	Ni thin film (if any)	Adsorption

3.3 Adsorption:

The adsorption phenomenon is a very important reference to nanoscience and environment in this very modern era in the field of surface phenomena i.e. adsorption.

(i) Physical adsorption:

ZnO particles have a negative zeta potential of -23.6 mV, indicating a negatively charged surface (Figure 3.19). Thein *et al.* (2015) attributed this negative charge to ZnO particles' OH^- groups. These OH^- groups adsorb actively. As shown in Figure 3.20(a), ZnO particle OH^- groups reacted with heavy metal cations in the aqueous solution to form a thin layer. Wang *et al.* (2010) noted this behavior. Adsorption efficacy was modest and ultimately saturated. Because visible light cannot encourage ZnO particles to produce electrons and holes, they physically adsorb metal ions from the solution.

(ii) Photogenerated electron-hole pair reduction/oxidation:

The metal's redox potential must exceed the conduction band (CB) level for ZnO particles to reduce. Ag (I), Cr (VI), and Cu (II) should potentially decrease. According to Litter *et.al. (*2009), metal ions will be preferentially oxidized if the oxidation potential is negative relative to VB. Pb (II) and Mn (II) ions oxidized. In Figure 3.20 (b), a suitable optical excitation source produces huge quantities of electrons and holes for metal ion reduction and oxidation. Thus, metal/metal oxide particles may be found in solution or as a thin coating over ZnO particles.

In conclusion, depending on the metal ions and light source, ZnO particles extracted heavy metal ions via one of the above procedures or a combination. In 15 minutes, visible light eliminated Cu (II) ions (Figure 3.1(a)). Absorption of Cu (II) ions into $Cu(H_2O)_6^{2+}$ ions, which subsequently interacted with OH^- ions through Lewis interaction, may have generated the CuO layer (Wang *et al.*, 2010). ZnO particle photocatalyst reduced Cu (II) ions under UV light (Bard *et al.*, 2017).

Visible-light-induced photoreduction of Ag (I) was implausible because the excited energy was insufficient to provide electrons for the ZnO catalyst. Thus, Ag^+ ions absorbed into the ZnO surface caused the low Ag (I) elimination in these circumstances. In Eq., ZnO's energy level, ee CB, is lower than Ag^+/Ag^0's redox potential. ZnO particles produce electrons when optically stimulated. After Ag (I) ions drew electrons from ZnO particles, the metal was deposited. During removal, UV light damaged Cd (II) and Ni (II) ions less than others (Ruvarac-Bugar *et al.*, 2005; Chenthamarakshan *et al.*, 2000; Quaranta *et al.*, 2017).

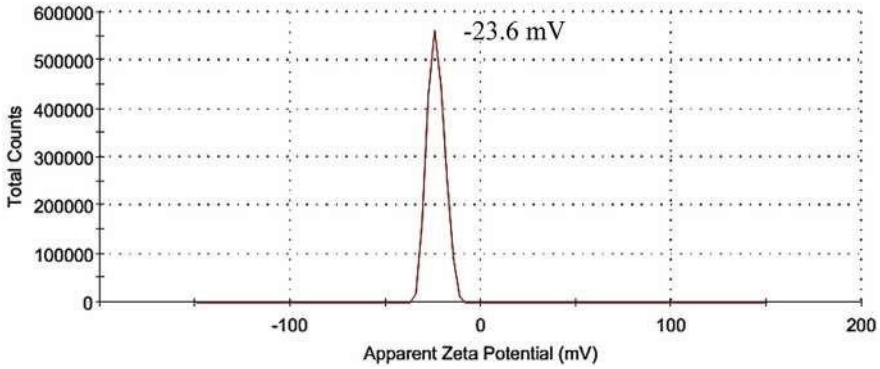

Figure 3.19. Zeta potential analysis reveals that ZnO particles have a positive surface charge.

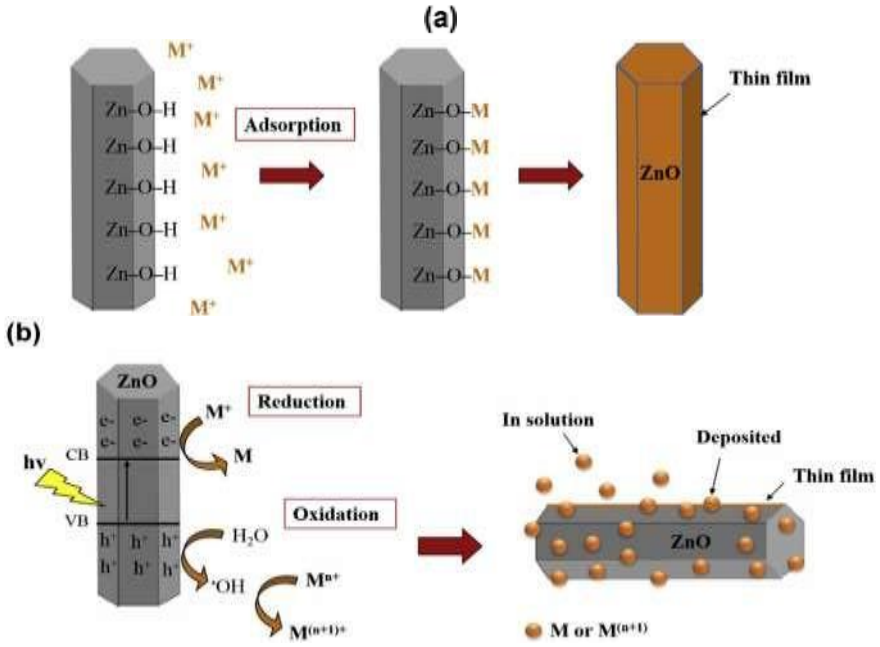

Figure 3.20. ZnO particles may effectively remove heavy metal ions by (a) adsorption and (b) a reduction/oxidation process.

The data of the samples analysis before the adsorption on nanoparticles are given in Table 3.3 and Figure 3.21, while after adsorption on nanoparticles, they are given in Table 3.4 and Figure 3.22.

Table 3.3. Samples analysis of Dams waters in Balochistan through Inductively Coupled Plasma for the extraction of Heavy Metals before adsorption on nano particles of ZnO.

Sample No	Name of Site Of Sample	Ag mg/l	Cdmg/i	Cr mg/l	Cumg/l	Mnmg/l	Nimg/l	Pbmg/l
1	Sabakzai Dam	0.0071	0.0021	0.016	0.005	0.003	ND	1.5
2	Hub Dam	0.0065	0.13	0.017	0.3	0.44	0.03	4.9
3	Mirani Dam	0.0065	0.07	0.15	0.2	0.1	0.02	1.6
4	Akara Kaur Dam	0.0063	0.102	0.16	0.03	0.09	,01	1.9

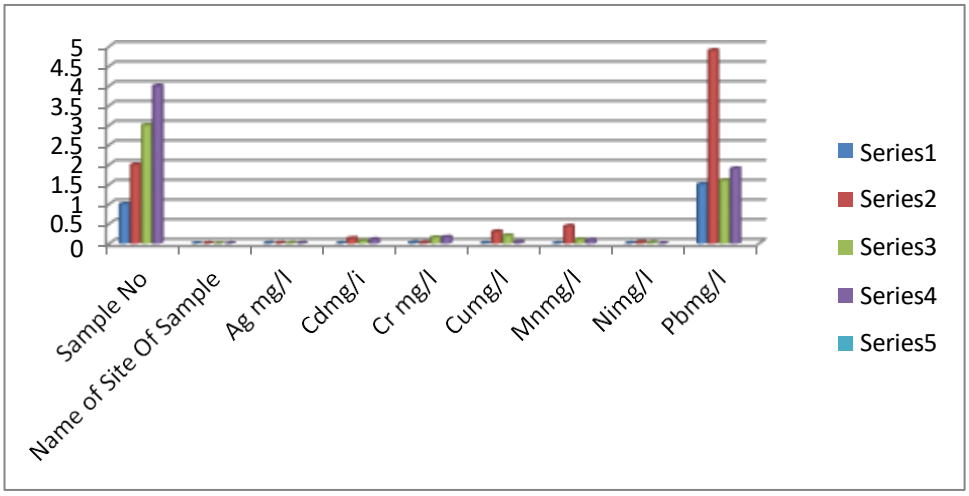

Figure 3.21. Samples analysis of Dams waters in Balochistan through Inductively Coupled Plasma for the extraction of Heavy Metals before adsorption on nano particles of ZnO.

Table 3.4. Samples analysis of Dams waters in Balochistan through Inductively Coupled Plasma for the extraction of Heavy Metals after adsorption on nano particles of ZnO.

Sample No	Name of Site Of Sample	Ag mg/l	Cdmg/l	Crmg/l	Cumg/l	Mnmg/l	Nimg/l	Pbmg/l
1	Sabakzai Dam	0	0	0	0	0	0	0
2	Hub Dam	0	0	0	0	0	0	0
3	Mirani Dam	0	0	0	0	0	0	0
4	Akara Dam	0	0	0	0	0	0	0

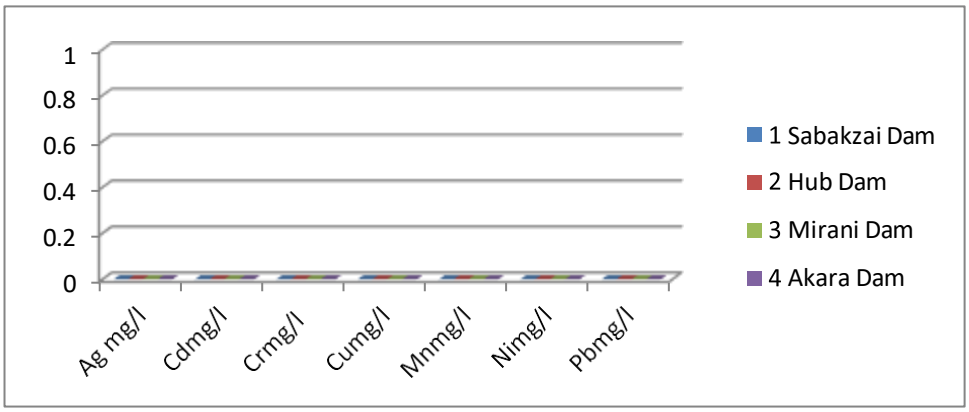

Figure 3.22. Samples analysis of Dams waters in Balochistan through Inductively Coupled Plasma for the extraction of heavy Metals after adsorption on nanoparticles of ZnO.

The figures 3.21&3.22 show that while the dam's water quality is good enough for drinking and domestic use, some modest treatments are still necessary to remove pollutants, especially alkalinity. It is also suggested that the water from the dam be slightly unsafe for human consumption. The efforts made in this experimental research may be beneficial in achieving the aims since the residents of that region are becoming more conscious of the need to preserve the higher quality and purity level of the dam water.

Nevertheless, research indicates that the study region's water quality from the dam is being negatively impacted by geogenic and anthropogenic factors. The study also demonstrated that the main source of ions in the waters of the experimental area under study is mineral weathering.

There are no flaws or mistakes, and the province's economy cannot support the waste of resources because of Pakistan's economic problems and the province of Balochistan's dearth of technology. Across the world, there are many examples of dam failures brought on by arid catchment areas that produce silty runoff.

3.4 Sustainability for Irrigation use

It was feasible to assess if subsurface water met the water needs of crops by using the sodium adsorption ratio. The sodium adsorption ratio is very important to plant growth because of its magnitude, which indicates the quantity of soil pore water accessible to plant roots (Wei *et. al.*, 2008). It is suitable for irrigation when the ratio of sodium adsorption to water is lower. Elevated salinity during irrigation might potentially affect the soil's aeration, permeability, infiltrations, structures, and flow rate. The sodium adsorption ratio for each subsurface water specimen in the district, derived from the mean of the data, ranges from 5 to 25. The underground water in the district would be utilized for irrigation, as stated by Richards (1954). This is really how vital nutrients like phosphate and nitrogen are not restricted. The total specimens were distributed uniformly, yet they could all be categorized as Good to Doubtful based on the values of the sodium adsorption ratio.

Conclusion

Under UV radiation, ZnO particles have shown significant effectiveness in extracting ions (Cr (VI), Pb (II), Ag (I), and Cu (II), but only moderately effective extraction of ions (Ni (II), Cd (II), and Mn (II). Three ions, such as Ag (I), Cr (VI), and Cu (II), were mostly removed by reduction, while two ions, (Mn (II) and Pb (II), were removed through oxidation. Contrarily, Cd (II) and Ni (II) ions were eliminated by adsorption when exposed to UV radiation. Instead of using a well-established reduction method, heavy metal ion extraction by ZnO particles was reliant on the kind of metal ion and the light source. According to the findings, ZnO particles are useful for treating wastewater that contains Cu (II), Ag (I), Pb (II), and Cr (VI) ions. Additionally, ZnO-based heavy metal ion sensors

might be created by using ZnO particles to selectively monitor heavy metal ions under various light sources.

Recommendations

At the result of this research, there are several proposal may be advised for the solution of the problem of the pollution of heavy metals in dam waters in light of our research.

● Before using the dam water for the purposes of drinking/cooking the facilities of the purification should be developed for the removal of Heavy Metals which will be granted any detrimental health impact on customers.

● There should be awareness of cleanliness of dams water reference to the usage of pesticides and manures for the purposes of the avoiding of the additional pollution of dam waters which is very significant to safe dam water and that will not endanger human health.

References

1. Bard, AllenJ. (2017). *Standard potentials in aqueous solution*. Routledge https://doi.org/10.1201/9780203738764
2. Barakat, M. A.(2011a), New Trends in Removing Heavy Metals from Industrial Wastewater.*Arab. J. Chem.*, 4 (4), 361-377.
3. Chenthamarakshan, C. K. Rajeshwar, E.J. Wolfrum (2000) Heterogeneous photocatalytic reduction of Cr (VI) in UV-irradiated titania suspensions: effect of protons, ammonium ions, and other interfacial aspects, Langmuir 16, 2715e2721.
4. Duffus, J. H (2002,). "Heavy Metals"- A Meaningless Term? (IUPAC Technical Report). *Pure Appl. Chem.. 74 (5),* 793-807.
5. Foster, W. (1936) Inorganic Chemistry (Niels Bjerrum). J. *Chem. Educ.*, 13 (7), 349.
6. Fu, F. Wang, Q. (2011). Removal of Heavy Metal Ions from Wastewaters: A Review. J. *Environ. Manage. 92 (3),* 407-418.
7. Guozhong, *C.(* 2004).*Nanostructures & Nanomaterials;* Imperial College Press.
8. Hashim, M. A.; Mukhopadhyay, S.; Sahu, J. N.; Sengupta, B.(2011). Remediation Technologies for Heavy Metal Contaminated Groundwater. J. *Environ. Manage.92 (10),* 2355-2388.
9. Jadhav, S. V; Bringas, E.; Yadav, G. D.; Rathod, V. K.; Ortiz, I.; Marathe, K. V.(2015), Arsenic and Fluoride Contaminated Groundwaters: A Review of Current Technologies for Contaminants Removal. J. *Environ. Manage. 162,* 306-325.
10. Kammerer, J.; Carle, R.; Kammerer, D. R. (2011). Adsorption and Ion Exchange: Basic Principles and Their Application in Food Processing. J. *Agric. Food Chem., 59 (1),* 22-42.
11. Litter M.I., (2009) Treatment of chromium, mercury, lead, uranium, and arsenic in water by heterogeneous photocatalysis, Adv. Chem. Eng. 36, 37e67.
12. Lofrano, G. (2012.). *Emerging Compounds Removal from Wastewater;*, Ed.; Springer Briefs in Molecular Science; Springer Netherlands: Dordrecht,
13. Munawar, K. M.A. Mansoor, W.J. Basirun, M. Misran, N.M. Huang, M. Mazhar, (2017) Single step fabrication of CuOeMnOe2TiO2 composite thin films with improved photoelectrochemical response, RSC Adv. 7, 15885e15893.
14. Nordberg, G. F., Fowler, B. A., Nordberg, M., Friberg, L. T.(2007). *Handbook on the Toxicology of Metals,* Third Edit.; Eds.; Academic Press Inc.
15. Ozin, G. A.; Arsenault, A. C.(2006). Nanochemistry: A Chemical Approach to Nanomaterials.*Small,* 2 (5), 678-679.
16. Patterson, J. M., & McCubbin, H. I. (1987). *Adolescent Coping Orientation for Problem Experiences (ACOPE)* [Database record]. APA PsycTests. https://doi.org/10.1037/t01546-000
17. Pokrpivny, *V. V.;* Skorokhod, *V. V.(* 2008) New Dimensionality Classifications of Nanostructures. *Phys. E Low-Dimensional Syst. Nanostructures, 40 (7),* 2521-2525.

18. Pollard, S.J.T., Thompson, F.E., McConnachie, G.L. (1994). Microporous carbons from Moringa Oleifera husk for water purication in less developed countries. Water Res., 29(1), 337-347.
19. Quaranta, V. M. Hellstr€om, J. r. Behler (2017) Proton-transfer mechanisms at the watereZnO interface: the role of presolvation, J. Phys. Chem. Lett. 8, 1476e1483.
20. Richards, L.A. 1954 Diagnosis and improvement of saline and alkali soils. Agricultural hand book 60. U.S. Dept. of Agriculture, Washington D.C., 160 p.
21. Roduner, E. (2006). Size Matters: Why Nanomaterials Are Different. *Chem. Soc. Rev.35,* 583- DOI: 10.1039/B502142C.
22. Ruvarac-Bugar~ci~c, I.A. Z.V. Saponjic, S. Zec, T. Rajh, J.M. Nedeljkovic (2005), Photocatalytic reduction of cadmium on TiO2 nanoparticles modified with amino acids, Chem. Phys. Lett. 407, 110e113.
23. Thein, M.T. S.-Y. Pung, A. Aziz, M. Itoh, (2015) Stacked ZnO nanorods synthesized by solution precipitation method and their photocatalytic activity study, J. Sol. Gel Sci. Technol. 74, 260e271.
24. Tressaud, A (2006), *Fluorine and the Environment : Atmospheric Chemistry, Emissions, & Lithosphere;* , Ed.; Elsevier.
25. Tu agua (2016) http://www.aigueshorta.es/ESP/16.asp (accessed Aug 28, 2016).
26. Wang, X. W. Cai, Y. Lin, G. Wang, C. Liang, (2010) Mass production of micro/nanostructured porous ZnO plates and their strong structurally enhanced and selective adsorption performance for environmental remediation, J. Mater. Chem. 20, 8582e8590.
27. Wei, X.; Kong, Y. L.; Hanfan, L.; Tao, H.; Chuntao, S.; Yanxi, Z. (2008) Microwave-assisted synthesis of nickel nanoparticles. *Mater. Lett.* 62, 2571.
28. WHO, (2011). "Guidelines for Drinking Water Quality 4th edition", Geneva.
29. Worch, E. (2012). *Adsorption Technology in Water Treatment - Fundamentals, Processes, and Modeling;* De Gruyter: Berlin/Boston,